Research Article

Hassan Yazdani, Mehdi Radmehr* and Alireza Ghorbani

# Innovative high-speed method for detecting hotspots in high-density solar panels by machine vision

https://doi.org/10.1515/ehs-2022-0100
Received August 13, 2022; accepted November 20, 2022;
published online December 5, 2022

**Abstract:** The occurrence of hotspots in photovoltaic panels is one of the most common problems of solar power plants, which reduces the output power of photovoltaic arrays and can also cause irreparable damage to the solar cells. There are several ways to identify hotspots, including using custom datasets using thermographic camera images, which will be later used to teach YOLO and Faster R-CNN computer vision algorithms. In practice, it is observed that the YOLO algorithm is many times faster than the Faster R-CNN in high-density solar panels. Therefore, the applied method is the safest choice for automatic hotspot detection in large-scale photovoltaic power plants to improve overall efficiency. In this paper, by comparing the performance of methods such as Faster R-CNN with YOLO, we concluded that the YOLO algorithm has far better advantages in terms of quality of detection, and speed. Therefore, this factor makes the use of YOLO significantly helps to speed up the troubleshooting of solar modules caused by hotspots, and this factor improves the efficiency of solar power plants in the long run. Meanwhile, in the studies for this paper, the results extracted by Python have been optimized as an algorithm to be used for hotspot detection.

**Keywords:** automatic hot spot detection; faster-RCNN; hot spot; YOLO.

## Introduction

Hot spot heating occurs when many photovoltaic cells are connected in series, and one cell produces a lower current than the rest of the cells for reasons such as defects in production, degradation, shading, or bad connections and junction failures. In such a situation, the output current of the solar panel is limited to that of the faulty cell (Kim et al. 2019; Moretón, Lorenzo, and Narvarte 2015).

HOT SPOTTING is a reliability problem in photovoltaic (PV) modules; this phenomenon is well-identified when a mismatched solar cell heats significantly and reduces the PV module output power (Ghanbari 2017). The hot spots are also the main cause of accelerated PV aging and sometimes irreversible damage to entire PV panels (Dhimish et al. 2018).

Production of current in healthy photovoltaic cells causes them to be forward biased and because in the short circuit, the terminal voltage is zero, the hot spotted cell is reverse biased. This causes the hot spotted cells to act as power loads that dissipate heat instead of producing power. There are several other reliability issues affecting PV modules, such as PV module disconnection (Moon, Blaauw, and Phillips 2017).

## Hot spot phenomenon in solar arrays

In photovoltaic power plants, large solar arrays consist of parallel-series connections of a large number of photovoltaic cells. A combination of series and parallel connections may cause several issues in the array. For example, one array might be open-circuited. In this case, the corresponding current from the sum of strings in a hot spotted block will be less than the rest of the blocks. From an electrical point of view, this is the same as a mismatch between the cells in series. Therefore, even if the characteristics of all cells are the same and there is no shading on the panel, there is still a chance for the formation of hot spots (http://pvcdrom.pveducation.org/MODULE/HotSpot, 2020, validation data2).

***Corresponding author: Mehdi Radmehr**, Department of Electrical Engineering, Sari Branch, Islamic Azad University, Sari, Iran, E-mail: radmehr@iausari.ac.ir
**Hassan Yazdani and Alireza Ghorbani,** Department of Electrical Engineering, Sari Branch, Islamic Azad University, Sari, Iran, E-mail: hafezyazdani@gmail.com (H. Yazdani), arghorbani@iausari.ac.ir (A. Ghorbani)

# Affecting factors in the formation of hot spots

## Defects in production

Photovoltaic cells with defects might have a non-uniform density of current. This may occur because of defects in the material itself or errors during manufacturing (Deng et al. 2017). This causes a mismatch between currents in cells that results in decreased output power. Because the cells are in series, the total current is limited to the current of the cell producing the least amount. During the operation, the cells with defects heat and are prone to irreversible damage (Waqar Akram et al. 2020).

## Degradation

With the increasing tendency towards thinner panels, silicon wafers are more prone to crack development. These cracks may develop at any time during the panel's lifetime (Akram et al. 2019). They mostly start during the water production and develop further during the operation of the photovoltaic panel. These cracks cause a mismatch in the produced current of the cells and in return cause dissipation of the power produced by healthy cells (Li et al. 2018).

## Shading

Hot spots resulting from external agents such as shading of trees or birds, etc., and soiling are usually temporary, because the source of the hot spots may be removed after a while. For example, the shadow of a tree moves at different hours of the day. Shading is one of the most common causes of hot spots (Hanifi, Schneider, and Bagdahn 2015).

## Junction failures and bad connections

Junction boxes connect the strings of photovoltaic cells and the output terminals. Also, junction boxes contain a diode for each string of photovoltaic cells. Bad connections and soldering can cause high resistance between the terminals, diodes, and cells. This high resistance can cause heat and, in turn, Hot spots.

# Consequences of hot spots

Since hot-spotted cells are reverse biased, they dissipate the power produced by the healthy cells (Moretón et al. 2014; Waqar Akram et al. 2019). This reduces the efficiency and the output power of photovoltaic cells. It also accelerates the degradation process of the hot spotted cells. The damages are usually irreversible and can even lead to the complete replacement of the solar panels.

# Methods of diagnosing and managing hot spots

## Bypass diodes

Most photovoltaic cell brands use a bypass diode with opposite polarity for the cells and parallel to the cell modules. Hence if a cell is shaded, it will be cut off from the circuit.

In Figure 1 the reverse current of a photovoltaic cell is shown. When the saturation current of the diode is increased, the $R_{sh}$ is reduced (Yang et al. 2010). Normally the photovoltaic cells are forward biased, and the bypass diode is reverse biased and no current flows through the diode. When a cell has an issue and its output current is reduced, it will become reverse biased, which in turn causes the bypass diode to be forward biased. The current

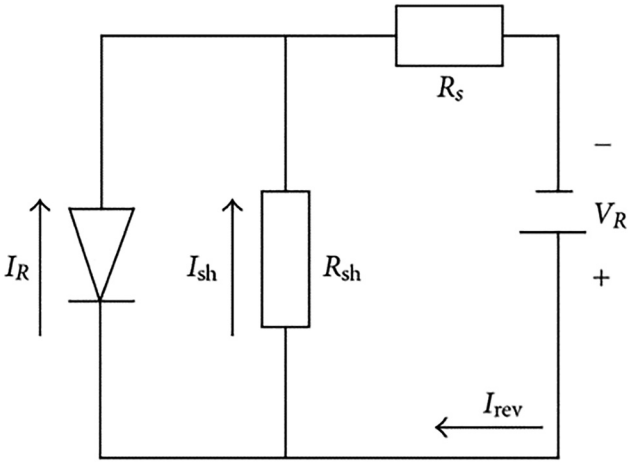


**Figure 1:** Reveres bias in a photovoltaic cell (Yang, Wang, and Wang 2012).

produced by healthy modules flows through the bypass, diode and the hot spotted region is cut off (Figure 2).

## The heat effect

Photovoltaic panels have a better performance at lower temperatures. Their output power is much higher in lower temperatures rather than in higher degrees. When a photovoltaic panel is subjected to sun rays, it heats up. Most of this heat is due to the absorption of infrared radiation. This increase in the panel's temperature is significant. We know from experience that the surface temperature of photovoltaic panels can reach up to 100°C. Most manufacturers of photovoltaic panels accommodate users with information about the heat effect on the performance of the photo-voltaic panel. In this information, a factor is introduced that is known as the temperature coefficient of the nominal output power of a photovoltaic cell. It is reported as a percentage of power reduction per each centigrade degree of temperature increase. In Figure 3, the effect of the increase of ambient temperature on the V–I characteristics of a panel is shown. As demonstrated, with temperature increase, the current increases as well but by such a small amount that it can be neglected. However, with the temperature increase, the output voltage is dropped significantly. The output power is the product of voltage and current, and as seen in Figure 3, with an increase in temperature, the output power is decreased (Moshtagh Dezfoli and Roshandel 2015). Evaluation of the output power can also be a useful method for the identifying of hot spots.

There are several methods in the identification of hot spots, such as identification by AC signal injection, light projection, and by infrared imaging with thermo-vision. Currently, the best method for identifying hot spots is infrared thermal imaging which is usually supervised by operators to detect possible defects in the panels.

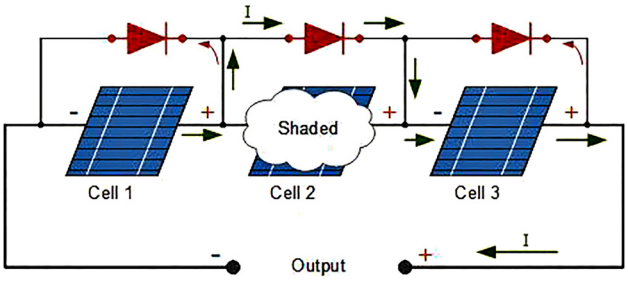


**Figure 2:** Function of the bypass diode during the occurrence of hot spot (https://www.alternative-energytutorials.com/photovoltaics/bypass-diode.html/, 2021, validation data3).

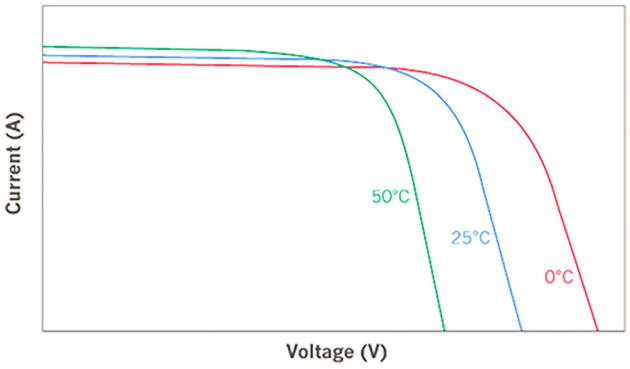


**Figure 3:** The effect of temperature increase on panel performance (Moshtagh Dezfoli and Roshandel 2015).

# Methods of hot spot imaging

Image processing is the processing of implementing different algorithms on an image to obtain the required information. One of the most significant problems we face while detecting hot spots in large-scale power plants is a large number of images; because, there is plenty of panels in the power plant, we need a large number of pictures from different panels. Therefore, several cameras are needed, which increases the cost of the project. To lower the costs, several methods are introduced, such as hot spot detection by projector (Wang et al. 2017) and thermal imaging by drone (Henry et al. 2020).

## YOLO[1] algorithm

First, let us start with the word YOLO. YOLO means that humans can easily understand what objects are in a picture, where they are, and how they relate to each other, but this process is very difficult for a computer (Redmon et al. 2016). In this research, after receiving the pictures and applying the required graphical processing, it is revealed that with the help of the YOLO algorithm, unified and automated monitoring can be conducted. Because in power plants with a high density of photovoltaic panels, high accuracy and low error are required, it is hard for a human operator to detect and distinguish errors quickly.

1 You look only once.

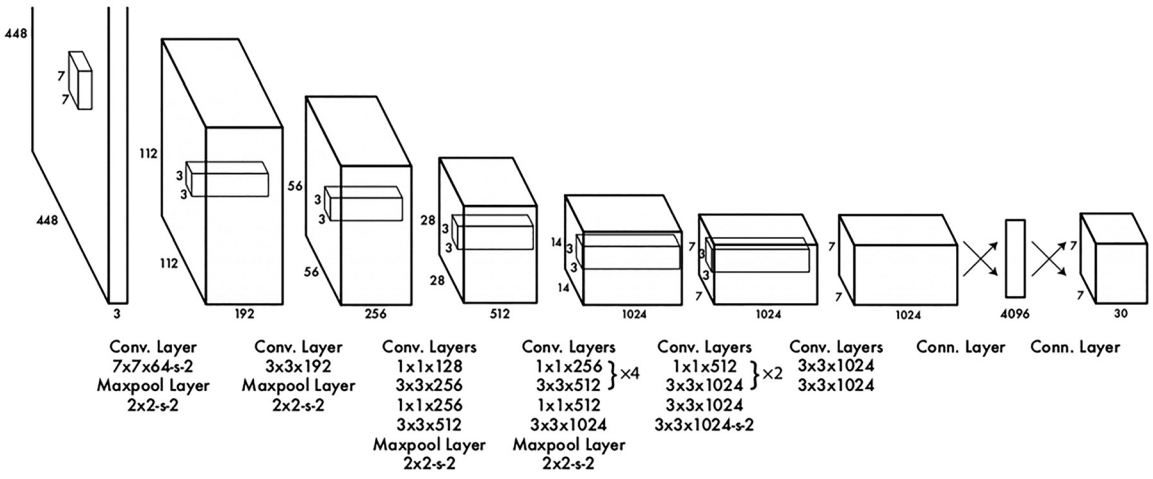


**Figure 4:** Overview of the layers of YOLO architecture (Redmon et al. 2016).

For the task of image processing, a few basic functions were first selected that are commonly used in graphic programs on PC and sometimes in features of commercial electronics (Kotyza and Kasik 2016).

YOLO employs a 24-layer Convolutional Neural Network for feature extraction and two fully connected layers for predicting items and their coordinates on the image. Figure 4 shows the architecture of the YOLO algorithm.

The use of convolutional neural networks (CNN, CONVnet) instead of standard classification algorithms is a trend in the research area of human detection, regardless of whether the task is nighttime detection using thermal imaging cameras or daytime detection using standard optical cameras. Thermal images are mainly used to detect the presence of people at night or in bad lighting conditions. However, they can perform poorly in the daytime when there is insufficient thermal contrast between the people and their surroundings (Ghose et al. 2019).

The development of CNNs helped move surveillance systems to embedded devices like the Raspberry Pi. Khalifa, Badr, and Elmahdy (2019).

Super-pixel refers to an irregular pixel block with a certain visual representation which consists of adjacent pixels with similar characteristics such as texture color, brightness, and so on (Achanta et al. 2012).

## Loss function of YOLO algorithm

With the increase in panel density in photovoltaic power plants, the Mean Squared Error (MSE) Function of the YOLO algorithm can be utilized. Because optimizing this loss function is easy and compatible with the regression problem in the YOLO algorithm. However, some changes need to be made to the MSE before it can be used in object detection according to the requirements, see equation (1);

$$\begin{aligned}
&\lambda_{\text{coord}} \sum_{i=0}^{S^2} \sum_{j=0}^{B} 1_{ij}^{\text{obj}} \left[ \left( x_i - \hat{x}_i \right)^2 + \left( y_i - \hat{y}_i \right)^2 \right] + \lambda_{\text{coord}} \sum_{i=0}^{S^2} \\
&\times \sum_{j=0}^{B} 1_{ij}^{\text{obj}} \left[ \left( \sqrt{w_i} - \sqrt{\hat{w}_i} \right)^2 + \left( \sqrt{h_i} - \sqrt{\hat{h}_i} \right)^2 \right] + \sum_{i=0}^{S^2} \\
&\times \sum_{j=0}^{B} 1_{ij}^{\text{obj}} \left( C_i - \hat{C}_i \right)^2 + \lambda_{\text{noobj}} \sum_{i=0}^{S^2} \sum_{j=0}^{B} 1_{ij}^{\text{noobj}} \left( C_i - \hat{C}_i \right)^2 \\
&+ \sum_{i=0}^{S^2} 1_i^{\text{obj}} \sum_{c \in \text{classes}} \left( p_i(c) - \hat{p}_i(c) \right)^2 . \qquad (1)
\end{aligned}$$

In this function $\hat{x}_i$, $\hat{y}_i$, $\hat{w}_i$, and $\hat{h}_i$ are the coordinates of the object located in the image that is already given to the algorithm, and the algorithm must be trained accordingly; $\hat{x}_i$ and $\hat{y}_i$ are the coordinates of the center of the object in the cell $i$.

$\hat{w}_i$ and $\hat{h}_i$ are the width and height of the bounding box that contains the object. $\hat{C}_i$ is the confidence of an object existing in cell $i$. $\hat{p}_i(c)$ is the existence probability of the object belonging to class $c$ in cell $i$. The values without (^) are the values extracted by the algorithm during each repetition in the training phase that is compared to the values given to the algorithm (also known as ground truths) and result in the loss function.

$1_i^{\text{obj}}$ shows if there is an object in cell $i$, and $1_{ij}^{\text{obj}}$ shows that the predictor box $j$ is responsible for the prediction.

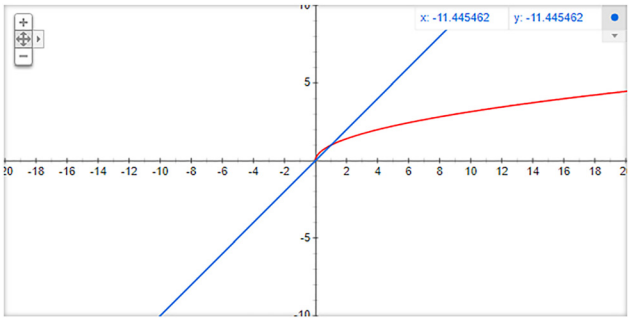


**Figure 5:** Comparison of a variable and the square root of a variable (https://howsam.org/yolo-algorithm/, 2021, validation data4).

However, there are some problems with this function. In the MSE loss function, the loss from localization and classification error has the same weight, which reduces the accuracy. Also, in every picture, most cells do not contain any objects. This causes the confidence score of these boxes to be zero and overwhelm the cells that contain an object and leave them neglected. This causes model instability. This also means that instead of converging the amount of error, which suggests the end of the training, the error values diverge and disrupt the learning of the neural network. To solve this issue, we increase the loss of localization while reducing the loss of confidence rating, and to realize this, we set ($\lambda_{\text{coord}} = 5$) and ($\lambda_{\text{noobj}} = 0.5$).

Also, in MSE, the weight of the error is the same in large and small boxes. At the same time, small errors in larger boxes should be reflected in less than the same number of errors in small boxes. In other words, a minor error in a large box should be less punishable than the same error in a smaller box. That is why we used the square root for the width and height of the bounding boxes, as seen in Figure 5.

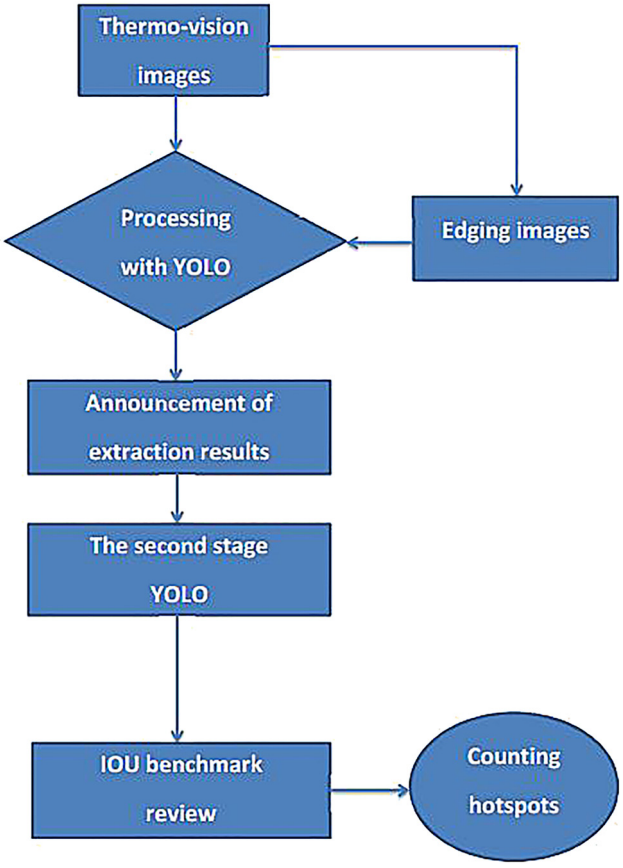


**Figure 7:** Flowchart of the automated hot spot detection process.

YOLO network is trained with Train and Validation data from PASCAL VOC 2007 and 2012 database (Figure 6). While testing on PASCAL VOC 2012 database, PASCAL VOC 2007 test data is also used for training (http://host.robots.ox.ac.uk/pascal/VOC/voc2007, 2007, Validation data1).

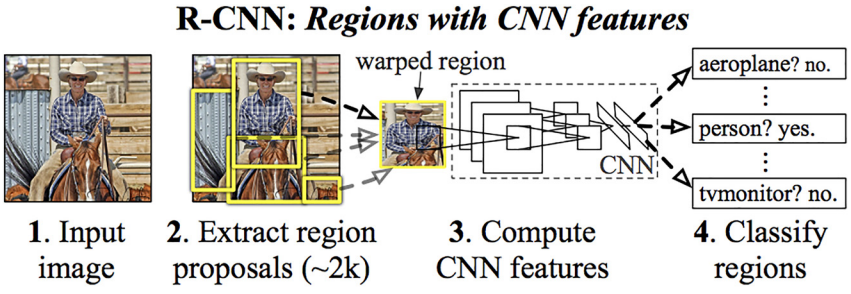


**Figure 6:** Overview of the detection process of R-CNN algorithm (Girshick et al. 2014).

### R-CNN[2] algorithm

R-CNN is a relatively older method of object detection. In this algorithm, around 2000 regions are proposed. Each of these regions passes the convolutional neural network and is classified. This means that to detect the objects in a picture, the picture has to pass through the neural network 2000 times (Girshick et al. 2014).

## Materials and methods

In this study, by using thermographic pictures obtained from the photovoltaic power plant, we try to detect hotspot events on solar panels in a large power plant complex. We can also determine the number of hot spots in real-time on the videos captured by FLIR E75 cameras which allows the operator to find the location and number of hot spots easily. The flowchart of the processing steps in this study is as follows (Figure 7):

As shown in Figure 7, in this innovative method, in order to detect the hot spot, the thermo-vision image is first entered into the system from thermal cameras. Then the image is entered into YOLO after edging. One of the reasons for taking the edge of the image and separating the parameters in the image in two colors, black and white, is to increase the processing speed; and after that, the number of hotspots is counted, and this step is repeated in two cycles to check the accuracy of operations. The important point, however, is that in this algorithm, you cannot use edge editing. Instead, it is possible to process the images in color in YOLO, which is suitable for power plants with a low number of solar panels. To edit the image, as shown in Figure 8, the first feature measures the difference in the light intensity between the hotspot area and the black area. The value of this property is obtained by adding the pixels in the upper black area and subtracting it from the pixel values in the white area.

According to Equation (2), the first feature measures the difference in light intensity between the hotspot area and the black area.

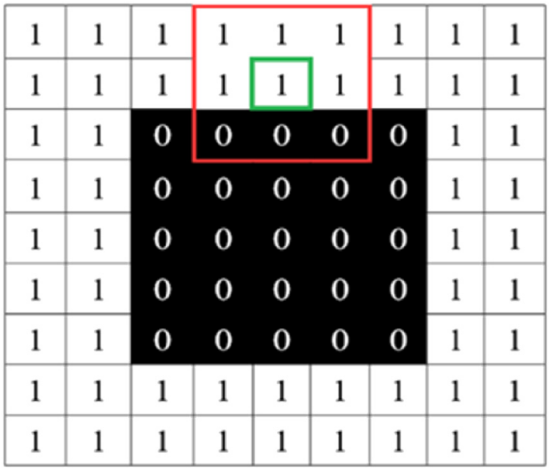


**Figure 8:** An example image of a hotspot area.

The value of this property is obtained by adding the pixels in the upper black area and subtracting it from the pixel values in the white area.

$$\text{Rectangle Feature} = \sum(\text{Pixels}_{\text{blackarea}}) - \sum(\text{Pixels}_{\text{whitearea}}) \quad (2)$$

One of the most useful tools in image processing is the Python programming language. The flexibility and portability of Python allow you to use this language on a variety of platforms in the industry, such as Windows, Linux, Macintosh, Solaris, etc.

### IOU[3] benchmark review

This criterion measures the degree of overlap between two "regions"; This value is equal to the area resulting from the overlap of these two areas, divided by the area resulting from the union of these two areas. This criterion shows the quality of the predictions produced by the object detection system compared to the correct answers of the ground truth. It compares them with each other, which is extracted according to relationship number (3).

$$\text{IoU} = \frac{\text{Area of overlap}}{\text{Area of Union}} \quad (3)$$

### Benchmark relationship IOU

The accuracy measure calculates the percentage of positive predictions that are correctly predicted as positive. The accuracy measure also calculates the ratio of "True Positives" to all possible outputs. The values of the precision and recall criteria are included in equations number (4) and (5), which are based on the predicted classes of false positives and true positives. It is that in Figure 9, the accuracy criterion function is drawn in a classified manner, which includes the final result of the performance accuracy for us, based on the final F1 relationship (equation number (6)), which is embedded in the Yolo processing algorithm. These two criteria have an inverse relationship with each other, which is shown in Figure 9.

$$\text{Recall} = \frac{\text{TP}}{\text{TP} + \text{FN}} \quad (4)$$

$$\text{Precision} = \frac{\text{TP}}{\text{TP} + \text{FP}} \quad (5)$$

$$F1 = 2^{\star}\frac{\text{Precision}^{\star}\text{Recall}}{\text{Precision} + \text{Recall}} \quad (6)$$

Validation and validation of accuracy: data related to checking the correctness of the performance of the YOLO-based machine vision algorithm with Train and Validation data from the PASCAL VOC 2007

| | Unpredicted Class | |
|---|---|---|
| Real Class | Positive | Negative |
| Positive | True Positive | False Negative |
| Negative | False Positive | True Negative |

**Figure 9:** Anticipated classes.

2 Region-Based Convolutional Neural Networks.

3 Intersection over Union.

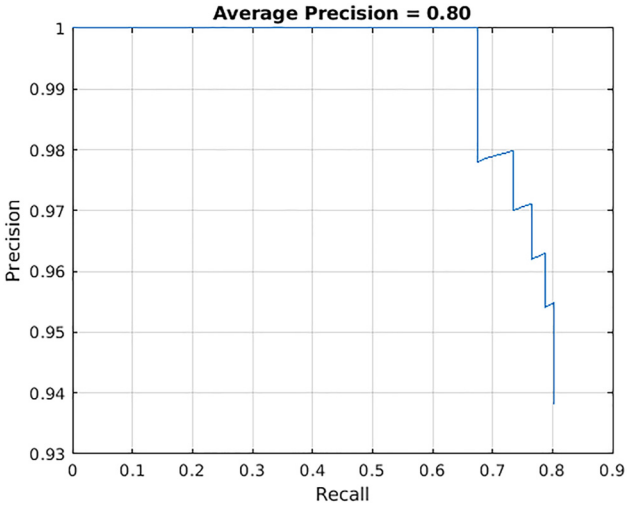


**Figure 10:** The average precision simulated function with YOLO version 3.

and 2012 database and thermo-vision images of real defective panels for simulation in MATLAB to implement object detector evaluation functions to measure common criteria. Such as the average precision (valuateDetectionPrecision) and the average error rates (evaluateDetectionMissRate) of the presentation are used. Average accuracy provides a single number that combines the detector's ability to classify (precision) correctly and the detector's ability to find all relevant objects (recall). Figure 10 is the average precision simulated function.

In this study, we compared two object detection methods in detect hotspots accurately. The first method is Faster-R-CNN, which is a slower method but, according to the articles, is more accurate at low density. The second method is the YOLO algorithm, which is faster but slightly less accurate at low densities.

In this study, we investigate the speed and accuracy of these two algorithms with the data set related to solar panel hot spots. It is worth noting that the same data set was used to train both algorithms, and the image file format was JPEG in the training and testing phases.

To utilize these algorithms, we must first train the convolutional neural network and obtain certain weight and configuration files that contain the information required by the network to detect a certain object. Then by employing these files, we use the neural networks to detect hot spots in pictures the networks have never seen before.

### Comparison of YOLO and faster R-CNN

This algorithm also needs high processing power for its training, and the convolutional neural network of this algorithm is known as the darknet. In the Google Colab environment, we implemented the code related to learning this algorithm and started training the algorithm. The algorithm reached proper accuracy in the training phase after 2220 repetitions, which took about 6 h.

It can be seen in Figure 14 that the input picture includes 10 hot spots. While YOLO did not detect one hot spot, it reported nine. However, Faster-R-CNN has reported eight hot spots because it counted three hot spots as one.

However, the Faster-R-CNN has serious problems in this regard. It is observed in Figure 15 that the Faster-R-CNN has performed badly in detecting small hot spots while the YOLO has detected them very well.

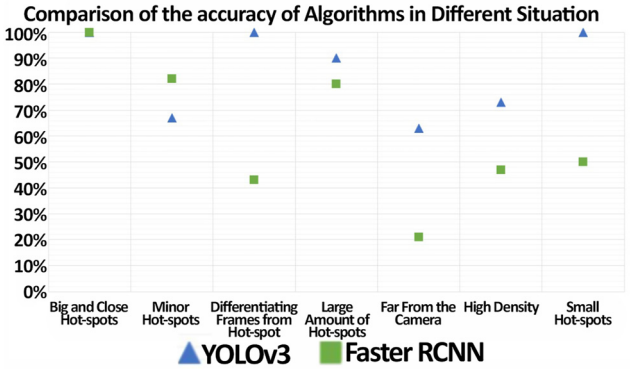


**Figure 11:** Comparison of the accuracy of the algorithms.

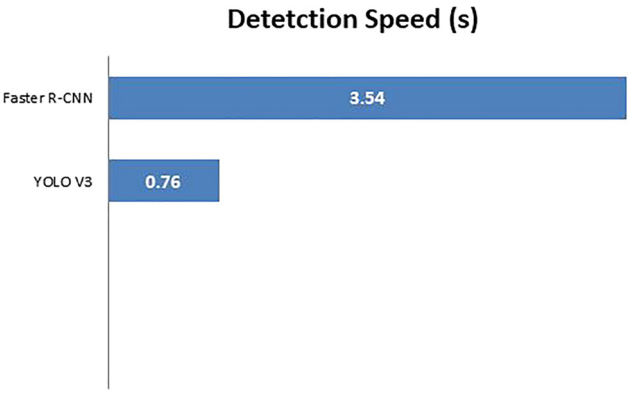


**Figure 12:** Comparing the detection speed of the algorithms.

Furthermore, the Faster-R-CNN's error in detecting the frame instead of the hot spot is very obvious. However, the YOLO has done it flawlessly. Figure 11 shows a comparison of these algorithms in accuracy.

In the training phase, using Google Colab's Tesla T4 graphics card, Faster-R-CNN took less time to train, about 3 h. However, YOLO needed 6 h for it to be trained. The speed results are shown in Figure 12. It is worth noting that the detection speed of the algorithms is not dependent on the input image. It means that it takes the same amount of time to perform detection on an image with four hot spots as it takes on an image with 10 hot spots or even no hot spots. This is why the speed is reported in a column chart.

## Results

As demonstrated, the YOLO algorithm with the hot spot data set possesses better precision and higher speed compared to the Faster-R-CNN. YOLO is more than four times faster than Faster-R-CNN. It would appear that YOLO is a suitable algorithm for deploying the automated identification of hot spots. While being faster and more accurate, YOLO requires less processing power which can reduce the project's costs.

The use of such algorithms in the automation of mundane and repetitive processes can be beneficial to both workers and the owners of photovoltaic power plants since almost no human supervision is required during the detection.

According to Table 1, the results of this research on hotspot diagnosis were evaluated by two different methods with 1500 images. Table 1 also illustrates the speed and accuracy of YOLO compared to FASTER-R-CNN and shows that in the improved method with YOLO, you can detect the hot spot defect with higher accuracy in addition to speed in high-density solar panels (Figure 13).

**Table 1:** Comparison results of hotspot detection performance in YOLO and Faster-R-CNN methods.

| Number of input images for processing | The output accuracy rate of faster-RCNN | The output accuracy rate of YOLO |
|---|---|---|
| 5 | 91% | 90% |
| 15 | 87% | 89% |
| 150 | 64% | 87% |
| 1500 | 57% | 89% |

## Discussion

The use of Python programming language for programming chips such as FPGA and Raspberry Pi is encouraged for deploying the results of computer vision for detecting hot spots in photovoltaic power plants. Because by simplifying the design process, it enables embedded system developers to take full advantage of the unique benefits of this algorithm in their applications.

## Conclusions

In this research, by introducing the hot spot phenomenon and evaluating the outcomes, we suggested different methods for identifying the hot spots, specifically the methods for automated detection by using computer vision. Furthermore, a detailed comparison of two of the most advanced object detection algorithms was presented, and it was shown that the YOLO algorithm, while being more accurate, also, is more than four times faster. Additionally, because the comparison was based on hot spots

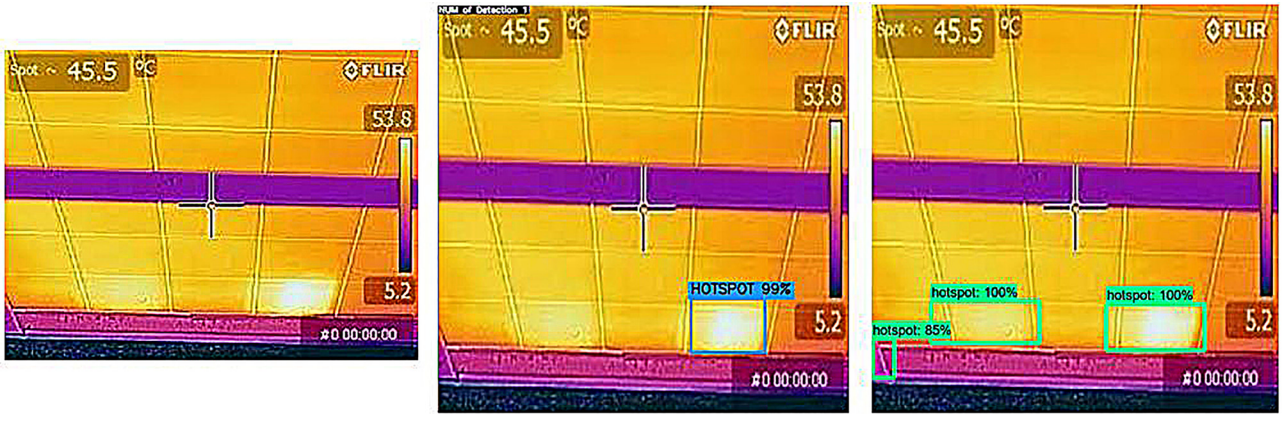


**Figure 13:** From left to right the input picture given to the YOLO algorithm's output, Faster R-CNN algorithm's output.

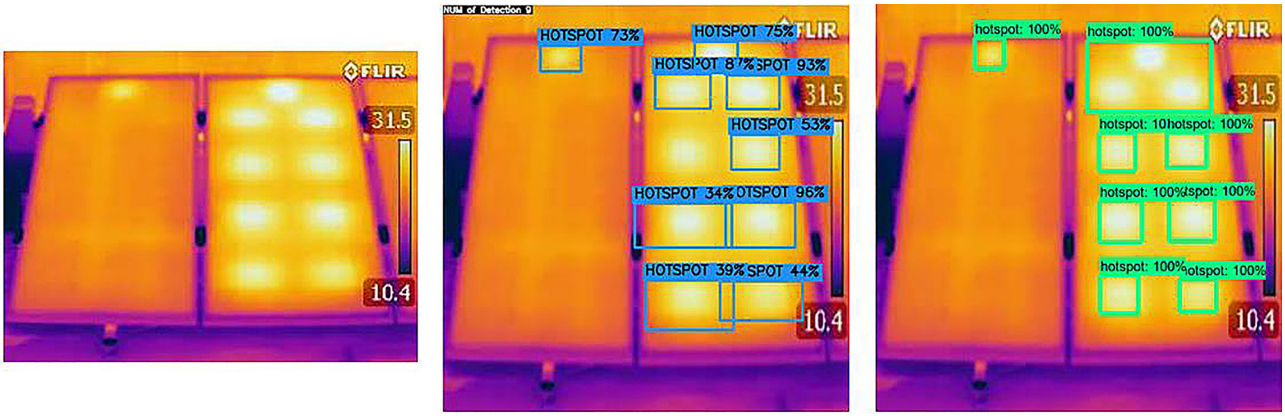


**Figure 14:** From left to right the input picture given to the YOLO algorithm's output, Faster R-CNN algorithm's output.


**Figure 15:** From left to right the input picture given to the YOLO algorithm's output, Faster R-CNN algorithm's output.

and not general objects such as cats or bicycles, it can help the designers and engineers working in this field to have a decent understanding of the subject since there is an increasing demand for photovoltaic power plants, maintaining these power plants take high priority. Specifically, the current project makes it possible for system architects, design engineers, and embedded systems programmers to implement a unified and integrated hot spot identification using the algorithms and methods discussed in this research.

**Acknowledgments:** We would like to thank the personnel of the Tavana Electronic Shomal corporate for helping us to gather the data and articles, particularly Mr. Rajabi Vandchali, for his dedication and support.
**Author contributions:** All the authors have accepted responsibility for the entire content of this submitted manuscript and approved submission.
**Research funding:** This research did not receive any specific grant from funding agencies in the public, commercial, or not-for-profit sectors.
**Conflict of interest statement:** The authors have no competing interests to declare that are relevant to the content of this article.
**Availability of data and material:** Raw data were generated at the Tavana Electronic Shomal large-scale facility. Derived data supporting the findings of this study are available from the corresponding author upon request.

## References

Achanta, R., A. Shaji, K. Smith, A. Lucchi, P. Fua, and S. Süsstrunk. 2012. "SLIC Superpixels Compared to State-of-the-Art Superpixel Methods." *IEEE Transactions on Pattern Analysis and Machine Intelligence* 34 (11): 2274–82.

Akram, M. W., G. Li, Y. Jin, X. Chen, C. Zhu, X. Zhao, A. Khaliq, M. Faheem, and A. Ahmad. 2019. "CNN Based Automatic Detection of Photovoltaic Cell Defects in Electroluminescence Images." *Energy* 189: 1–15.

Deng, S., Z. Zhang, C. Ju, J. Dong, Z. Xia, X. Yan, T. Xu, and G. Xing. 2017. "Research on Hot Spot Risk for High-Efficiency Solar Module." *Energy Procedia* 130: 77–86.

Dhimish, M., V. Holmes, P. Mather, and M. Sibley. 2018. "Novel Hot Spot Mitigation Technique to Enhance Photovoltaic Solar Panels Output Power Performance." *Solar Energy Materials and Solar Cells* 179: 72–9.

Ghanbari, T. 2017. "Permanent Partial Shading Detection for Protection of Photovoltaic Panels against Hot Spotting." *IET Renewable Power Generation* 11 (1): 123–31.

Ghose, D., S. M. Desai, S. Bhattacharya, D. Chakraborty, M. Fiterau, and T. Rahman. 2019. "Pedestrian Detection in Thermal Images Using Saliency Maps." In *Proceedings of the IEEE/CVF Conference on Computer Vision and Pattern Recognition Workshops*.

Girshick, R., J. Donahue, T. Darrell, and J. Malik. 2014. "Rich Feature Hierarchies for Accurate Object Detection and Semantic Segmentation." In *Proceedings of the IEEE Conference on Computer Vision and Pattern Recognition*, 580–7.

Hanifi, H., J. Schneider, and J. Bagdahn. 2015. "Reduced Shading Effect on Half-Cell Modules—Measurement and Simulation." In *31st European Photovoltaic Solar Energy Conference and Exhibition*, 2529–33.

Henry, C., S. Poudel, S.-W. Lee, and H. Jeong. 2020. "Automatic Detection System of Deteriorated PV Modules Using Drone with Thermal Camera." *Applied Sciences* 10 (11): 3802.

http://host.robots.ox.ac.uk/pascal/VOC/voc2007 (accessed April 2022).

http://pvcdrom.pveducation.org/MODULE/HotSpot.htm (accessed June 2020).

https://howsam.org/yolo-algorithm/ (accessed March 2021).

https://www.alternative-energytutorials.com/photovoltaics/bypass-diode.html/ (accessed July 2021).

Kim, H., D. Xu, C. John, and Y. Wu. 2019. "Modeling Thermo-Mechanical Stress of Flexible CIGS Solar Cells." *IEEE Journal of Photovoltaics* 9 (2): 499–505.

Kotyza, J., and V. Kasik. 2016. "Image Processing of Composite Video with FPGA Programmable Logic." *IFAC-PapersOnLine* 49 (25): 482–6.

Khalifa, A. F., E. Badr, and H. N. Elmahdy. 2019. "A Survey on Human Detection Surveillance Systems for Raspberry Pi." *Image and Vision Computing* 85: 1–13.

Li, G., Y. Jin, M. Akram, X. Chen, and J. Ji. 2018. "Application of Bio-Inspired Algorithms in Maximum Power Point Tracking for PV Systems under Partial Shading Conditions–A Review." *Renewable and Sustainable Energy Reviews* 81: 840–73.

Moretón, R., E. Lorenzo, and L. Narvarte. 2015. "Experimental Observations on Hot Spots and Derived Acceptance/Rejection Criteria." *Solar Energy* 118: 28–40.

Moon, E., D. Blaauw, and J. D. Phillips. 2017. "Subcutaneous Photovoltaic Infrared Energy Harvesting for Bio-Implantable Devices." *IEEE Transactions on Electron Devices* 64 (5): 2432–7.

Moretón, R., E. Lorenzo, J. Leloux, and J. M. Carrillo. 2014. "Dealing in Practice with Hot Spots". arXiv preprint arXiv:1411.0621.

Moshtagh Dezfoli, M., and R. Roshandel. 2015. "Study of the Effect of Temperate on the Output Power of Photo-Voltaic Panels in Solar Power Systems." In *1st International Conference on Research in Science and Technology*.

Redmon, J., S. Divvala, R. Girshick, and A. Farhadi. 2016. "You Only Look Once: Unified, Real-Time Object Detection." In *Proceedings of the IEEE Conference on Computer Vision and Pattern Recognition*, 779–88.

Wang, Y., K. Itako, T. Kudoh, K. Koh, and Q. Ge. 2017. "Voltage-based Hot Spot Detection Method for Photovoltaic String Using a Projector." *Energies* 10 (2): 230.

Waqar Akram, M., G. Li, Y. Jin, C. Zhu, A. Javaid, M. Z. Akram, and M. U. Khan. 2020. "Study of Manufacturing and Hotspot Formation in Cut Cell and Full Cell PV Modules." *Solar Energy* 203: 247–59.

Waqar Akram, M., G. Li, Y. Jin, X. Chen, C. Zhu, X. Zhao, M. Aleem, and A. Ahmad. 2019. "Improved Outdoor Thermography and Processing of Infrared Images for Defect Detection in PV Modules." *Solar Energy* 190: 549–60.

Yang, H., H. Wang, and M. Wang. 2012. "Investigation of the Relationship between Reverse Current of Crystalline Silicon Solar Cells and Conduction of Bypass Diode." *International Journal of Photoenergy*, https://doi.org/10.1155/2012/357218.

Yang, H., W. Xu, H. Wang, and M. Narayanan. 2010. "Investigation of Reverse Current for Crystalline Silicon Solar Cells—New Concept for a Test Standard about the Reverse Current." In 35th IEEE Photovoltaic Specialists Conference.